ACS APPLIED MATERIALS & INTERFACES

Research Article

www.acsami.org

Shape Memory Performance of Thermoplastic Polyvinylidene Fluoride/Acrylic Copolymer Blends Physically Cross-Linked by Tiny Crystals

Jichun You, Hui Fu, Wenyong Dong, Liping Zhao, Xiaojun Cao, and Yongjin Li*

College of Material, Chemistry and Chemical Engineering, Hangzhou Normal University, No. 16 Xuelin Road, Xiasha High-tech Zone, Hangzhou 310036, China

ABSTRACT: Polyvinylidene fluoride (PVDF)/acrylic copolymer (ACP) blends are a typical miscible crystalline/amorphous system over the whole composition range. Our previous investigation indicated that blend samples with controlled component ratios and crystallization conditions exhibit good shape memory properties (*J. Phys. Chem. B* **2012**, *116*, 1256−1264). In this work, we systematically investigated the cold crystallization temperature effects on the crystal morphologies and the shape memory properties for the 50/50 blend. It was found that the quenched blend is an amorphous material with a low glass transition temperature. Annealing at temperatures above T_g of the blend induces crystallization of PVDF from the miscible amorphous PVDF/ACP phase, leading to an increased glass transition temperature of the blend. High annealing temperature results in large PVDF spherulites, while low annealing temperature produces tiny crystals in the blend. Furthermore, tiny crystals serve as the physical cross-link points and the amorphous regions among them act as the reversible phase for the blend materials during the mechanical deformations. Therefore, the PVDF/ACP blends with tiny crystals show not only high shape fixity but also excellent recovery ratios.

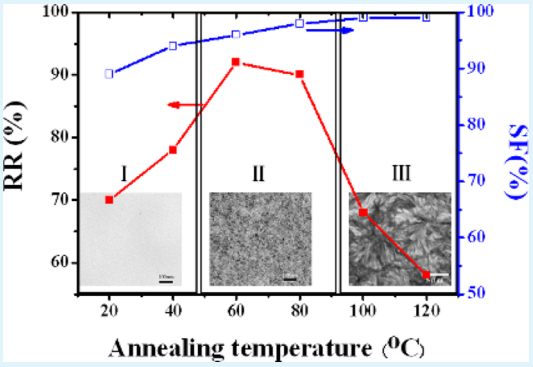

KEYWORDS: *shape memory properties, physical cross-link, cold crystallization, tiny crystals, polymer blend*

1. INTRODUCTION

Shape memory polymers (SMPs) are materials that can memorize and recover their original permanent shape from a temporary shape upon exposure to an external stimulus such as heat, light, moisture, chemical environment or magnetic field. SMPs have received increasing attention due to their low density, high deformation strain, good processability and tunable transition temperatures.[1−5] They exhibit potential applications in smart fabrics,[6] intelligent-medical devices,[7] and in the biomedical field, such as smart suture materials,[8] responsive stents for cardiovascular engineering,[9] self-expandable implants for minimally invasive surgery,[10] and controlled drug release.[11] On the molecular level, SMPs usually consist of at least two components: switching phases and permanent netpoints.[12−14] Switching phases act as molecular switches with well-defined melting temperatures (T_m) or glass transition temperatures (T_g) and enable the fixation of the temporary shape. The switching phase must be joined into a network structure linked by the net points (cross-linking points) to prevent stretched polymer chains from irreversibly sliding by one another during deformation. The cross-links are generally chemical bonds created by some special curatives leading to thermoset SMPs, for example, the γ-irradiation cross-linked PE[15,16] and peroxide-vulcanized polyolefine SMPs.[17,18] Such netpoints in shape memory network can also be physical aggregates, for instance, the glassy domains in a multiphase block copolymer.[19−22] Recently, Zhang et al.[23] reported a supramolecular shape memory materials based on an inclusion complex of polyethylene oxide and cyclodextrins (CDs), which is a thermoplastic SMP. All of these materials are either chemically cross-linked polymers lacking recyclability or block copolymers which are difficult to synthesize.

We have recently reported a new type of thermoplastic SMP from a miscible crystalline/amorphous polymer blend.[24] When the blend compositions of poly(vinylidene fluoride) (PVDF) and an acrylic copolymer are well controlled, the blend materials show unique deformation behavior and excellent shape memory performance. We proposed that the amorphous molecular chains bridge the tiny PVDF crystals to form a three-dimensional network, in which the small PVDF crystals act as the netpoints to prevent the deformed molecular chains from sliding during the mechanical deformation. Thermoplastic SMPs from miscible crystalline/amorphous polymer blends provide a new avenue to SMPs because the fabrication strategy is simple and widely applicable. More important, the prepared SMPs are thermoplastic and can be readily reused many times. However, the crystal morphological effects on the shape memory performance for such SMPs are not clear. In the present work, therefore, emphasis was placed on the cold crystallization condition effects on the structure and properties

Received: June 26, 2012
Accepted: August 17, 2012
Published: August 17, 2012

 © 2012 American Chemical Society

of the SMP. Our results indicate that high cold crystallization temperature results in large PVDF spherulites in the blend, while low cold crystallization temperature induces tiny crystals in the blend. It was further found that only the blends with tiny crystals exhibit high shape memory performance. The investigation is crucially important for the structural design of SMPs from a miscible crystalline/amorphous polymer blend.

2. EXPERIMENTAL SECTION

2.1. Materials and Sample Preparation. The PVDF and acrylic copolymer were kindly provided by Kureha Chemicals, Japan, and Nagase Co., Ltd., respectively. The molecular weight and polydispersity of the PVDF are M_w = 209 000 and M_w/M_n = 2.0, respectively, as determined by gel permeation chromatography. The acrylic copolymer is a ternary copolymer of acrylonitrile, ethylacrylate, and butylacrylate. The weight-average molecular weight of the acrylic copolymer is M_w = 287 000. The glass transition temperature of the acrylic copolymer is 56 °C, as measured by dynamic mechanical analysis. All of the polymers were dried in a vacuum oven at 80 °C for at least 12 h before processing. PVDF/acrylic copolymer blends (50/50) were prepared using a Brabender-type plastic mixer (Toyoseiki Co. KF70 V) with two rotors at a rotation speed of 100 rpm at 190 °C for 10 min. After blending, the samples were hot pressed at 200 °C for 5 min into a film with a thickness of 500 μm, followed by quenching in ice water. The quenched films were then annealed in an oven at different temperatures for 12 h for further characterization.

2.2. Structural Characterization. Wide-angle X-ray diffraction (WAXD) profiles were obtained using CuKα radiation (40 kV, 120 mA) generated by an X-ray diffractometer (Rigaku, Ultrax 8000) with a scanning speed of 1 deg/min. Differential scanning calorimetry (DSC) was carried out under nitrogen flow at a heating or cooling rate of 10 K/min with a Perkin-Elmer DSC-7 differential scanning calorimeter calibrated with the melting temperature of indium and zinc.

Dynamic mechanical analysis (DMA) was conducted with a RHEOVIBRON DDV-25FP (Orientec Corp.) in the tensile mode. The dynamic storage and loss moduli were determined at a frequency of 1 Hz and a heating rate of 3 °C/min as a function of temperature from −150 to 150 °C.

The structure of the PVDF/acrylic copolymer blend was characterized by transmission electron microscopy (TEM). Thin slices of samples were microtomed using a Reichert Ultracut S (Leica Microsystems Co. Ltd.) at −40 °C. The sections were collected onto a 600-mesh copper grid and were stained with RuO_4 at room temperature for 20 min. The TEM images were observed using a transmission electron microscope (Hitachi 7000) at an accelerating voltage of 75 kV.

2.3. Property Measurements. Tensile tests were carried out according to ASTM D 412−80 test method by using the dumbbell shaped samples punched out from the molded sheets. The tests were performed using a tensile testing machine, Tensilon UMT-300 (Orientec. Co., Ltd.), at a crosshead speed of 10 mm/min at 20 °C and 50% relative humidity.

The creep tests of the blends were performed at a temperature of 30 °C with a stress level of 1 MPa using a TA Q800 Dynamic Mechanical Analysis (DMA) instrument (TA Instrument Inc.). After 2 h, the stress was released and the sample was allowed to recover for 1 h. The strain development was recorded as a function of time during the measurements.

Shape-memory property measurements were conducted according to the procedure shown in our previous work.[24] The specimen with an original length l_0 was first stretched to length l_1 at 75 °C and then quenched to 0 °C (the length was l_2 after quenching). The stretched sample was then heated to the 75 °C again and the length of the specimen was measured to be l_3. The recovery ratio (RR) and the shape fixity (SF) were defined as RR = $(l_2 - l_3)/(l_2 - l_0)$ and SF = $(l_2 - l_0)/(l_1 - l_0)$, respectively.

3. RESULTS

3.1. Morphologies of PVDF/Acrylic Polymer Blends. Figure 1 shows WAXD profiles of quenched PVDF/ACP and

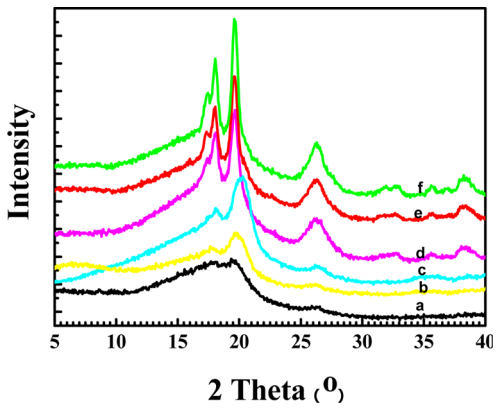

Figure 1. WAXD profiles for the PVDF/ACP blends with various thermal histories (a) quenched sample; (b) 40 °C cold crystallized sample; (c) 60 °C cold crystallized sample; (d) 80 °C cold crystallized sample; (e) 100 °C cold crystallized sample; and (f) 120 °C cold crystallized sample.

the cold crystallized blends at the indicated temperatures. A large and broad halo originating from the amorphous region is observed while small and broad diffraction peaks due to the crystalline region are only barely visible for the quenched blend. This means that the quenched sample is almost amorphous with very low crystallinity. The PVDF/acrylic copolymer is a thermodynamically miscible blend and the addition of amorphous polymers decreases the overall crystallization rate of PVDF. When the quenched samples are annealed at the temperature above T_g, part of PVDF molecules from the amorphous PVDF/ACP region crystallize, so the diffraction peaks can be observed for the cold crystallized blends. With increasing cold crystallization temperatures, the diffraction intensity increases and diffraction peak becomes more narrow, indicating increased crystallinity and enlarged crystal size. Note that all PVDF crystallizes into the α-crystal phase[25] independent of the annealing temperatures.

TEM images for the quenched and the cold crystallized blends are displayed in Figure 2. Note that the scale for the last image is different from that of the first two. No component domain can be observed in any of the TEM images, indicating the miscible state between PVDF and acrylic copolymer. WAXD results have shown that the quenched sample is almost amorphous with very low crystallinity. From the TEM image, it is also seen that the quenched blend is homogeneous without any detectable structure. However, the annealing at 60 °C induces observable PVDF crystals in the cold crystallized blend. Many thin and short crystal lamellae are seen from the TEM image (Figure 2b). All of these tiny crystals are less than 100 nm in length, and these nanosized crystals do not affect the transparency of the materials, as further described in section 3.3. When the sample was annealed at 120 °C, totally different crystal morphologies are obtained. The PVDF forms spherulite structures with the diameter ranging from 2 to 10 μm (Figure 2c). The results by TEM measurements are highly consistent with those obtained using WAXD characterization.

3.2. Thermal Behaviors. Figure 3 displays the DSC thermograms during heating for the quenched and cold

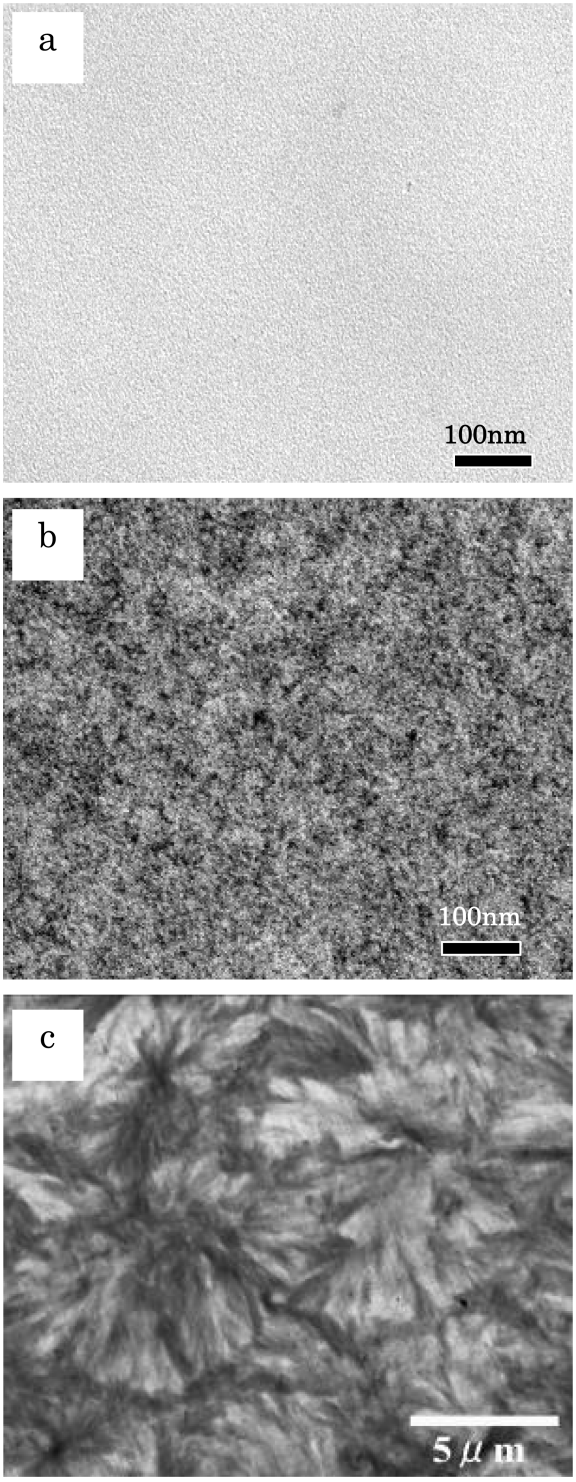

Figure 2. TEM images of PVDF/ACP blends (a) quenched sample; (b) cold crystallized at 60 °C; and (c) cold crystallized at 120 °C (note that the scale is different for the last image with the first two).

crystallized PVDF/acrylic copolymer blends. Quenched sample and the 40 °C annealed sample show similar heating behavior with one exothermic peak due to the cold crystallization (T_c) observed at 90−110 °C before melting of the crystallites, whereas for samples annealed above 60 °C, only the melting peak is observed. For the sample annealed at 40 °C, the annealing temperature is just above T_g of the sample, so the crystal growth rate is slow because of the difficulty in the

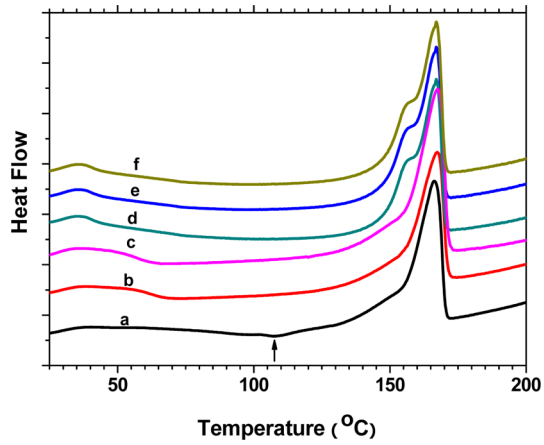

Figure 3. DSC thermograms during heating for (a) quenched sample; (b) 40 °C cold crystallized sample; (c) 60 °C cold crystallized sample; (d) 80 °C cold crystallized sample; (e) 100 °C cold crystallized sample; and (f) 120 °C cold crystallized sample.

diffusion of the crystalline segments; with an increase in the temperature, however, the diffusion is easier and complete crystallization occurs, showing an exotherm. In the other annealed sample, the crystallization is almost complete and no exotherm is observed. The DSC results indicate that the annealing cannot lead to the full crystallization of PVDF when the annealing temperature is lower than 60 °C. On the basis of these DSC data, the crystallinity (X_c) of each specimen was estimated from the following equation

$$X_c = 100(\Delta H_m - \Delta H_c)/\Delta H_f \quad (1)$$

where ΔH_m, and ΔH_c are respectively the enthalpies of melting and of cold crystallization. Here, the value of ΔH_f, the heat of fusion, defined as the melting enthalpy of 100% crystalline PVDF, was taken to be 90.4 J/g from the literature.[26] The calculated crystallinity for each sample is tabulated in Table 1. The increased cold crystallization temperature results in gradually enhanced crystallinity. No drastic enhancement in crystallinity was observed for the samples upon annealing at the temperature higher than 60 °C. The crystallinity of the 120 °C annealed samples is only about 5% higher than that of the 60 °C annealed sample. We concluded that low-temperature annealing leads to the sample with many more crystals of smaller size, which can also be observed in the TEM image (Figure 2b). The high concentration of tiny crystals is crucial for the high shape memory performance.

The storage moduli (E') of the quenched and cold crystallized PVDF/acrylic copolymer are summarized in Figure 4A. The E' value of quenched blend decreases significantly as the temperatures increase from 15 to 40 °C, followed by an obvious increase in the storage modulus. The drastic decrease in the modulus is attributed to the glass transition, while the following modulus enhancement above the glass transition temperature is due to the cold crystallization of PVDF during the heat-scanning processes. In contrast, no modulus enhancement for the cold crystallized samples was observed during heating because most of the PVDF crystals formed during the annealing. However, the dynamic mechanical properties of the cold crystallized samples are much dependent on the cold crystallization temperatures. With increasing cold crystallization temperature, the storage modulus increases greatly above room

Table 1. Crystallinity, Storage Modulus at 25 °C, and the Glass Transition Temperature of the PVDF/ACP Blends Crystallized at Different Temperatures

sample	quenched	40 °C	60 °C	80 °C	100 °C	120 °C
crystallinity (%)	8.9	12.5	42.7	43.6	47.3	47.8
glass transition temp. (°C)	31.8	36.5	45.6	46.3	49.1	50.5
storage modulus at 25 °C (MPa)	207	704	2106	2131	2102	2429

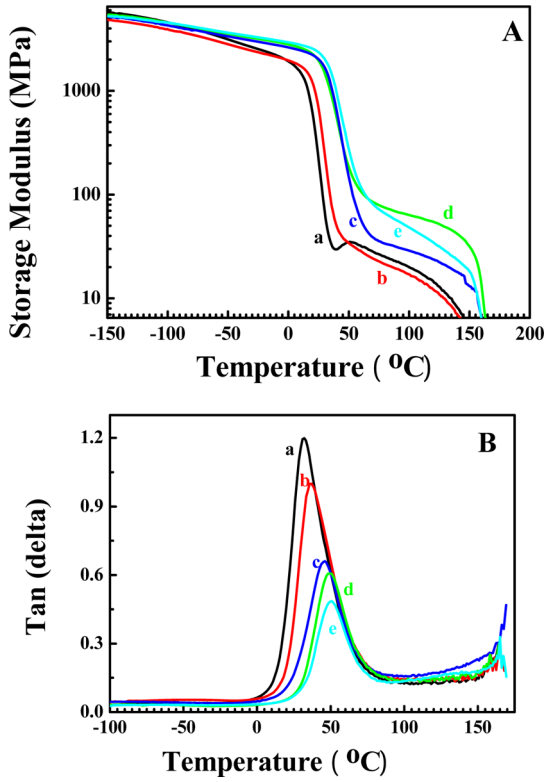

Figure 4. (A) Storage modulus and (B) tan (delta) profiles for the PVDF/ACP blends with various thermal histories (a) quenched sample; (b) 40 °C cold crystallized sample; (c) 60 °C cold crystallized sample; (d) 100 °C cold crystallized sample; and (e) 120 °C cold crystallized sample.

temperature, as shown by the storage modulus values of the samples at room temperature (25 °C), tabulated in Table 1.

Figure 4 (B) shows the dynamic loss of the quenched and cold crystallized samples. Only one sharp relaxation peak was observed for all samples, indicating that PVDF and acrylic copolymer are miscible in the amorphous region at the molecular level and no phase separation occurs because of the cold crystallization. On the other hand, the cold crystallization temperature affects the glass transition temperature significantly. The relaxation peak temperatures are also shown in Table 1. The T_g of the quenched sample is ca. 32 °C, whereas that of the sample annealed at 120 °C increases to 50.5 °C. The Fox equation has been widely used to predict T_g of a miscible polymer blend as follows[27]

$$\frac{1}{T_g} = \frac{X_{PVDF}}{T_{g_{PVDF}}} + \frac{X_{ACP}}{T_{g_{AVP}}} \quad (2)$$

where T_g is glass transition of the blend, $T_{g_{PVDF}}$ and $T_{g_{ACP}}$ are the glass transition temperatures of neat PVDF and acrylic copolymer, respectively, X_{PVDF} and X_{ACP} are weight fractions of amorphous PVDF and acrylic copolymer, respectively. The T_g of neat PVDF is −40 °C and that of neat acrylic copolymer is 56 °C. In the crystalline polymer/amorphous polymer blends, the X_{PVDF} and X_{ACP} should be calculated by taking only the amorphous fraction of the crystalline polymer into account.[28,29] With an increase in annealing temperature, this amorphous portion decreases and therefore the T_g of the blend increases.

Noted that the all samples display a very sharp glass transition in Figure 4B, which is required for a good SMP using the T_g as the switching temperature. On the other hand, the dependence of T_g on the annealing temperature provides an accessible strategy to adjust the switching temperature of the final SMPs, which has been one of important topics for SMPs research.[30−32] It is seen that for the sample crystallized at 60 °C, the T_g is ca. 45 °C. Below this temperature, the material is hard (storage modulus E' = 2.10 GPa at 25 °C), whereas above this temperature, it displays typical rubberlike elasticity (E' = 35 MPa at 75 °C), with very large maximum elongations. On the other hand, the switching temperature of the material is about 45 °C, which is not far from body temperature. This fact is very important because one of the most attractive applications of SMPs is in the medical field. We consider that the material has potential applications as the medical fixing parts, stents, or surgical sutures due to the excellent shape memory properties and its relatively low switching temperature.

3.3. Mechanical Properties. The cold crystallization temperature not only affects the morphology and crystallinity of the PVDF/ACP blend, but also has a great influence on the mechanical properties of the blend, as shown in Figure 5. The

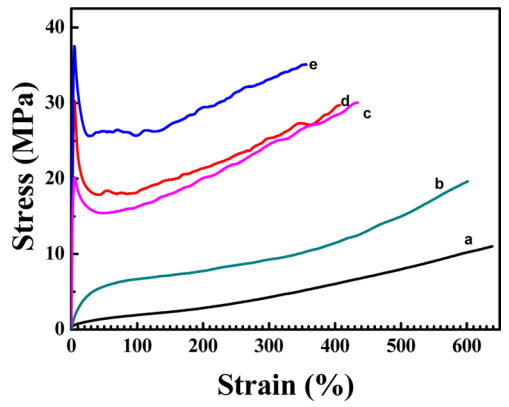

Figure 5. Strain−stress curves of PVDF/ACP blends cold crystallized under various temperatures: (a) quenched sample; (b) cold crystallized at 40 °C; (c) cold crystallized at 60 °C; (d) cold crystallized at 100 °C; and (e) cold crystallized at 120 °C.

strain−stress curves for all samples were measured at 25 °C. Quenched PVDF/acrylic copolymer is very soft and highly elongated. In fact, the quenched sample is in a rubbery state because the T_g of the quenched sample is about 32 °C, which is close to the measuring temperature. The annealed sample at 40 °C also shows typical stretching behaviors of a rubbery material

with no yielding and large elongation at break. However, both the modulus and the tensile strength are much higher than that of the quenched blend, which can be attributed to both the increased *Tg* and the enhanced PVDF crystal content. Totally different S−S curves are observed for the samples cold crystallized at temperatures of 60 °C or higher. All the blends show high modulus with clear yielding and strain-softening after yielding. In addition, all the samples break at relatively high elongation at break. When higher cold crystallization temperatures are employed, higher modulus and higher tensile strength are obtained.

Figure 6 shows photographs for PVDF/ACP samples with different thermal histories. The quenched sample is transparent

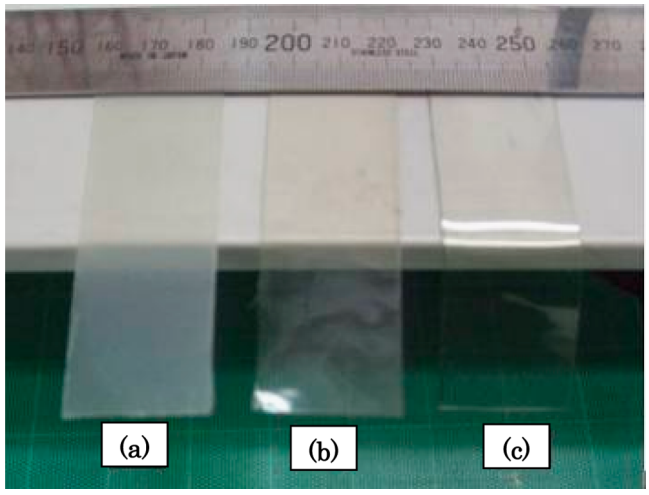

Figure 6. Photos of the PVDF/ACP blends cold crystallized under various temperatures: (a) cold crystallized at 120 °C; (b) cold crystallized at 60 °C; and (c) quenched sample.

and very soft. Annealing induces an improvement in the mechanical properties; thus the cold crystallized samples can be self-supported, as shown in Figure 6a, b. This result is consistent with the tensile measurements in Figure 5. Moreover, significant differences in the optical properties can also be observed for the samples undergoing thermal treatment. Like the quenched blend, the sample annealed at 60 °C is clear and shows high transparency. For the sample annealed at 120 °C, however, the film is opaque and exhibits low transmittance in the visible region. Such differences originate from the crystal size in the samples. The crystal size is in the nanoscale range in the sample annealed at 60 °C and the nanostructured inhomogeneity does not scarify the transmittance of the material. In contrast, the spherulites several micrometers in diameter induce the significant light scattering and refraction, so the sample annealed at 120 °C displays a totally different appearance with the quenched and 60 °C annealed samples.

The cold crystallization effects on the creep behaviors have been investigated. Figure 7 shows the creep behavior of the PVDF/ACP blends annealed at different temperatures at 30 °C. It is seen that the quenched sample shows very large instantaneous deformation and remnant deformation after releasing the stress. This is obviously attributed to the low glass transition temperature and lacking the cross-link points in the quenched sample. Therefore, the molecular slip occurs upon the long-term stress. In contrast, the annealed samples show typical creep behavior of rigid plastics. It is interesting to find that the sample annealed at 60 °C exhibits better anticreep

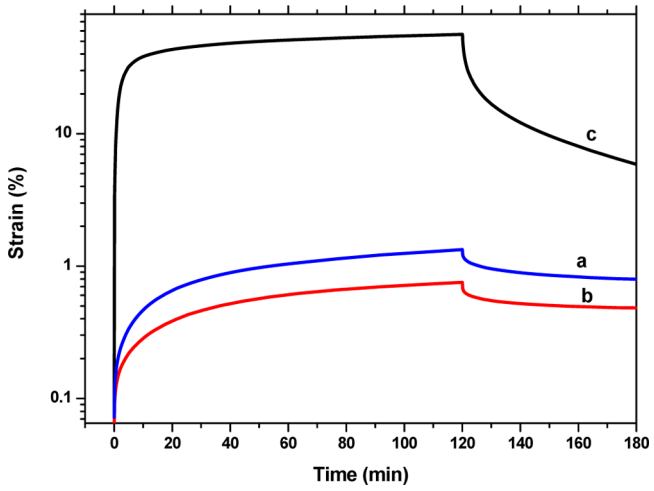

Figure 7. Creep curves of the PVDF/ACP blends cold crystallized under various temperatures: (a) cold crystallized at 120 °C; (b) cold crystallized at 60 °C; and (c) quenched sample.

behavior and better elastic recovery upon the stress releasing than the sample annealed at 120 °C. This result indicates that the sample annealed at 60 °C will present better shape memory performance, as will be discussed in the following section.

3.4. Shape Memory Properties. Figure 8 shows the shape fixity (SF) and shape recovery ratio (RR) as a function of the

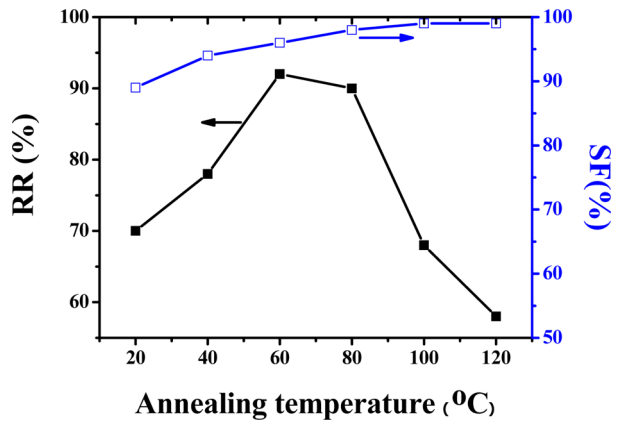

Figure 8. Shape recovery ratio (RR) and shape fixity of PVDF/ACP blends as function of the annealing temperatures at the deformation of 100% (the annealing temperature of 20 °C corresponds to the quenched sample).

cold crystallization temperature with the deformation ratio of 100%. It is seen that all samples show shape fixity higher than 90%. With increasing cold crystallization temperature, the shape fixity increases slightly. However, the recovery ratios of the PVDF/acrylic copolymer blends show strong cold crystallization temperature dependence. The highest recovery property is observed when the sample was annealed at 60 °C−80 °C. The RR is about 90% and the corresponding SF is approximately 95%, which are very close to those of the well-known polyurethane SMPs, indicating excellent shape memory performance of the blends. Further increase in cold crystallization temperature leads to a sudden drop in the recovery properties.

An example of the macroscopic shape memory effect of the cold crystallized PVDF/ACP blends is demonstrated in Figure

dx.doi.org/10.1021/am301161s | ACS Appl. Mater. Interfaces 2012, 4, 4825−4831

9. The quenched sample was annealed at 60 °C for 12 h with a spiral shape (Figure 9 A), which is the permanent shape of the

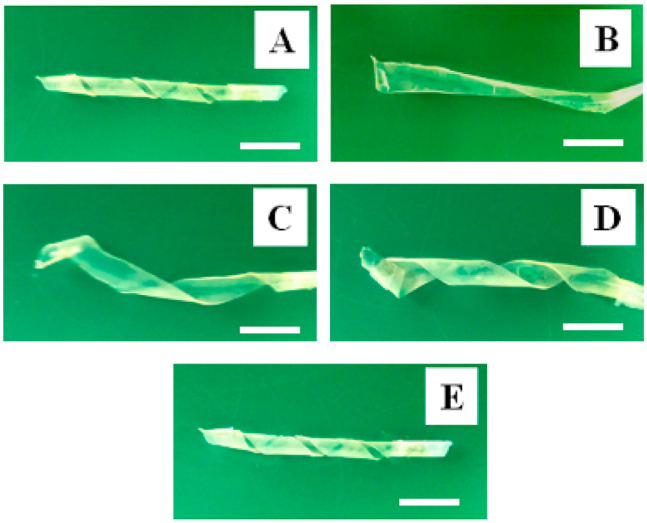

Figure 9. One shape memory cycle of the PVDF/ACP blends cold crystallized at 60 °C (scale bar is 1 cm for the all images).

sample. The spiral shaped sample was changed into a relatively flat belt at 60 °C, and then put into water at 20 °C to obtain the temporary shape (B). When placed into an environment of 60 °C, the sample quickly changed back to the original permanent spiral shape E via the stages of C and D. Note that this thermal mechanical deformation cycle can be performed many times, indicating that the SMPs show good shape memory stability.

4. DISCUSSION

It is clear that the cold crystallization temperature shows drastic effects on the morphology and shape memory properties of the PVDF/ACP blends. The quenched blends are almost amorphous with a glass transition temperature of about 32 °C. The material is soft and exhibits large mechanical deformation under external force. Part of the deformation cannot be recovered because of the molecular slip in this quenched amorphous sample. Therefore, the quenched sample displays a low value in both shape fixity and recovery ratio. The subsequent annealing of the quenched samples results in the crystallization of PVDF from the miscible state. PVDF crystallizes into spherulites several micrometers in diameter when it is annealed at high temperatures. Materials with big spherulites are rigid and display high tensile strength. The breaking of the spherulites by mechanical stretching results in a permanent deformation, which cannot be recovered by subsequent thermal treatment. Therefore, the shape recovery ratio is also small for the blends cold crystallized at high temperatures. For the samples that anneal at temperatures ranging from 60 to 80 °C, PVDF crystallizes from the amorphous state into very small crystals. The tiny crystals not only enhance the modulus and tensile strength of the material, but also take the role of the fixed phase to prevent the irreversible sliding of the molecular chains. Therefore, a high shape recovery ratio and a good anticreep behavior are achieved. The schematic diagram for the shape memory PVDF/ACP blends annealed at low temperature is shown in Figure 10. The small PVDF crystals act as physical cross-links in the materials and they drive the recovery of the polymer

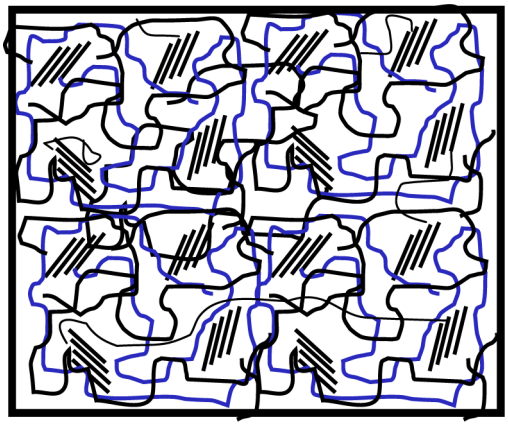

Figure 10. Morphological diagram for high-performance SMPs cross-linked by tiny crystals from a miscible crystalline/amorphous polymer blend (blue line indicates ACP chain, black line indicates PVDF chain, and the region with the paralleled black bars indicates the PVDF crystal with very small size).

during the shape memory cycle. When the deformed sample is cooled down again, the molecular chains between the PVDF crystals are frozen and vitrification occurs, so the shape is fixed. When the temperature is higher than T_g of the blend, the material is soft and readily deforms. The elongated chain recovers due to the entropy elasticity and high shape recovery ratio is achieved if the specimen was heated to a temperature higher than T_g.

5. CONCLUSION

In summary, we found that the morphology and the properties of miscible PVDF/ACP blends can be well controlled by the cold crystallization of a quenched amorphous blend. The samples cold crystallized at high temperature are rigid and opaque because of the large spherulites and high crystallinity. These samples exhibit low shape recovery ratio value due to the large irreversible deformation by the breaking of spherulites induced by the mechanical deformations. The tiny crystals less than 100 nm in length formed at the relatively low cold crystallization temperatures from the quenched amorphous blends act as the effective fixed phase to keep the permanent shape of the blend; thus high fixity and high shape recovery ratio can be achieved. The glass transition temperature of the molecular chains bridging the neighboring tiny crystals is the switching temperature for the obtained SMPs, which can be adjusted in a range of about 5 °C by the cold crystallization conditions. We consider that the obtained SMPs may be useful for the biomedical application since the switching temperature is very close to the body temperature.

AUTHOR INFORMATION

Corresponding Author

*E-mail: yongjin-li@hznu.edu.cn.

Notes

The authors declare no competing financial interest.

ACKNOWLEDGMENTS

This work was financially supported by the National Natural Science Foundation of China (21074029, 21104014, 51173036, 21104013) and Zhejiang Provincial Natural Science Foundation of China (R4110021). This work was also partially

supported by the Project of Zhejiang Key Scientific and Technological Innovation Team 2010R50017.

REFERENCES

(1) Gil, E. S.; Hunson, S. A. *Prog. Polym. Sci.* **2004**, *29*, 1173.
(2) Behl, M.; Razzaq, M. Y.; Lendlein, A. *Adv. Mater.* **2010**, *22*, 3388.
(3) Lendlein, A.; Kelch, S. *Angew. Chem., Int. Ed.* **2002**, *41*, 2034.
(4) Xie, T. *Nature* **2010**, *464*, 267.
(5) Wang, W.; Jin, Y.; Ping, P.; Chen, X.; Jing, X.; Su, Z. *Macromolecules* **2010**, *43*, 2942−2948.
(6) Mondal, S.; Hu, J. L. *Indian J. Text. Res.* **2006**, *31*, 66.
(7) El Feninat, F.; Laroch, G.; Fiset, M.; Mantovani, D. *Adv. Eng. Mater.* **2002**, *4*, 91.
(8) Lendlein, A.; Langer, R. *Science* **2002**, *296*, 1673.
(9) Metcalfe, A.; Desfaits, A.-C.; Salazkin, I.; Yahia, L. H.; Sokolowski, W. M.; Raymond, J. *Biomaterials* **2003**, *24*, 491.
(10) Yakacki, C. M.; Shandas, R.; Lanning, C.; Rech, B.; Eckstein, A.; Gall, K. *Biomaterials* **2007**, *28*, 2255.
(11) Wache, H. M.; Tartakowska, D. J.; Hentrich, A.; Wangner, M. H. *J. Mater. Sci.* **2003**, *14*, 109.
(12) Lendlein, A.; Schmidt, A. M.; Schroeter, M.; Langer, R. *J. Polym. Sci., A: Polym. Chem.* **2005**, *43*, 1369.
(13) Choi, N. Y.; Lendlein, A. *Soft Matter* **2007**, *3*, 901.
(14) Xie, T. *Nature* **2010**, *464*, 267.
(15) Kumar, S.; Pandya, M. V. *J. Appl. Polym. Sci.* **1996**, *64*, 823.
(16) Ota, S. *Radiat. Phys. Chem.* **1981**, *18*, 81.
(17) Kolesov, I. S.; Radusche, H.-J. *Express Polym. Lett.* **2008**, *2*, 461.
(18) Liu, C.; Chun, S. B.; Materh, P. T.; Zheng, L.; Haley, E. H.; Coughlin, E. B. *Macromolecules* **2002**, *35*, 9868.
(19) Skakalova, V.; Lukes, V.; Breza, M. *Macromol. Chem. Phys.* **1997**, *198*, 3161.
(20) Liu, C.; Qin, H.; Mather, P. T. *J. Mater. Chem.* **2007**, *17*, 1543.
(21) Ratna, D.; Karger-Kocsis, J. *J. Mater. Sci.* **2008**, *43*, 254.
(22) Vara, R.; Grant, C.; Daniel, C. *World Rubber* **2003**, *227*, 33.
(23) Zhang, S.; Yu, Z.; Govender, T.; Luo, H.; Li, B. *Polymer* **2008**, *49*, 3205.
(24) You, J.; Dong, W.; Zhao, L.; Cao, X.; Qiu, J.; Sheng, W.; Li, Y. *J. Phys. Chem. B.* **2012**, *116*, 1256.
(25) Salimi, A.; Yousefi, A. A. *Polym. Test.* **2003**, *22*, 699.
(26) Welch, G. J.; Miller, R. L. *J. Polym. Sci., Polym. Phys. Ed.* **1976**, *14*, 1683.
(27) Fox, T. G. *Bull. Am. Phys. Soc.* **1956**, *1*, 123.
(28) Hahn, B. R.; Herrmann-Schonherr, O.; Wendorff, J. H. *Polymer* **1987**, *28*, 201.
(29) Alfonso, G. C.; Terturro, A.; Pizzoli, M.; Scandola, M.; Ceccorulli, G. *J. Polym. Sci.* **1989**, *B27*, 1195.
(30) Xie, T. *Polymer* **2011**, *52*, 4985.
(31) Behl, M.; Razzaq, M. Y.; Lendlein, A. *Adv. Mater.* **2010**, *22*, 3388.
(32) Xie, T.; Xiao, X.; Cheng, Y.-T. *Macromol. Rapid Commun.* **2009**, *30*, 1823.